

Evidence of decoupled lattice distortion and ferroelectric polarization in the relaxor system PMN-xPT

Guangyong Xu,¹ D. Viehland,² J. F. Li,² P. M. Gehring,³ and G. Shirane¹

¹Physics Department, Brookhaven National Laboratory, Upton, New York 11973, USA

²Department of Materials Science and Engineering, Virginia Tech., Blacksburg, Virginia 24061, USA

³NIST Center for Neutron Research, National Institute of Standards and Technology, Gaithersburg, Maryland 20899, USA

(Received 8 October 2003; published 30 December 2003)

We report high q -resolution neutron scattering data on PMN-xPT single crystals with $x=20\%$ and 27% . No rhombohedral distortion occurs in the 20PT sample for temperatures as low as 50 K. On the other hand, the 27PT sample transforms into a rhombohedral phase below $T_C \sim 375$ K. Our data provide conclusive evidence that a phase with an average cubic lattice is present in the bulk of this relaxor system at low PT concentration, in which the ferroelectric polarization and lattice distortion are decoupled. The rhombohedral distortion is limited to the outermost tens of microns of the crystal.

DOI: 10.1103/PhysRevB.68.212410

PACS number(s): 77.80.-e, 77.84.Dy, 61.12.Ex

The complex perovskite system $\text{Pb}(\text{Mg}_{1/3}\text{Nb}_{2/3})\text{O}_3$ (PMN) is a close analog to $\text{Pb}(\text{Zn}_{1/3}\text{Nb}_{2/3})\text{O}_3$ (PZN), both of which have been studied extensively because of their extraordinary piezoelectric properties. The addition of PbTiO_3 (PT) enhances the piezoelectricity significantly, forming solid solutions PMN-xPT and PZN-xPT for $0 \leq x \leq 1$.^{1,2} This discovery has motivated numerous studies of the structural phase transitions in these systems as a function of x . The current zero-field phase diagrams of PMN-xPT and PZN-xPT share many common features, including a purported cubic-to-rhombohedral phase transition at small values of x (Refs. 2–4) (see Fig. 1). One exception to this is pure PMN ($x=0$), which is reported to retain an average cubic structure down to temperatures as low as 5 K.^{5,6} The rhombohedral distortions in both PMN-xPT and PZN-xPT have been observed directly by x-ray scattering experiments^{3,7,8} and related to the establishment of ferroelectric order in each system.

Several recent studies have now uncovered evidence of a different phase located on the rhombohedral side of the phase diagram. Electric-field studies of PZN-8PT by Ohwada *et al.*⁹ show that the unpoled system does not exhibit a rhombohedral unit-cell distortion below T_C . This was a hint that a different phase, which was labeled phase X, may exist there. Subsequent high energy x-ray structural studies by Xu *et al.*¹⁰ prove that the inside of single-crystal PZN has an undistorted lattice, providing conclusive evidence of this phase. While phase X has an average undistorted lattice ($a=b=c, \alpha=\beta=\gamma=90^\circ$), the true symmetry of the phase is still unknown. Motivated by these findings, Gehring *et al.*¹¹ performed neutron-scattering measurements with very fine q resolution on a single-crystal sample of PMN-10PT. In contrast to previous 8.9 keV Cu K_α x-ray measurements by Dkhil *et al.*¹² on a powder sample of the same compound, the neutron data show no evidence of a rhombohedral distortion below T_C , and are consistent with the presence of phase X.

In this paper we present high q -resolution neutron-scattering data on PMN-xPT with $x=20\%$ (20PT) and 27% (27PT), both of which are on the the $R(X)$ side of the phase

diagram (see Fig. 1). Our data show that these two compounds are notably different. One of them (20PT) exists as phase X at low temperatures, which has an undistorted lattice, inconsistent with the previously reported rhombohedral distortion by x-ray measurements on similar compounds.⁷ On the other hand, 27PT shows a clear rhombohedral distortion below $T_C \sim 375$ K. We believe that phase X is one in which an undistorted lattice is ferroelectrically polarized, and thus highly unusual. This decoupling breaks down with increasing PT concentration x , and allows the local atomic displacements to develop into a global rhombohedral phase.

Our samples are high quality single crystals of PMN-20PT and 27PT, having dimensions $3 \times 3 \times 3 \text{ mm}^3$ and $10 \times 3 \times 3 \text{ mm}^3$, respectively. Both of them have been de-poled before the neutron measurements. The neutron-scattering experiments were performed on the BT9 triple-axis spectrometer at the NIST Center for Neutron Research. Measurements were made using a fixed incident neutron en-

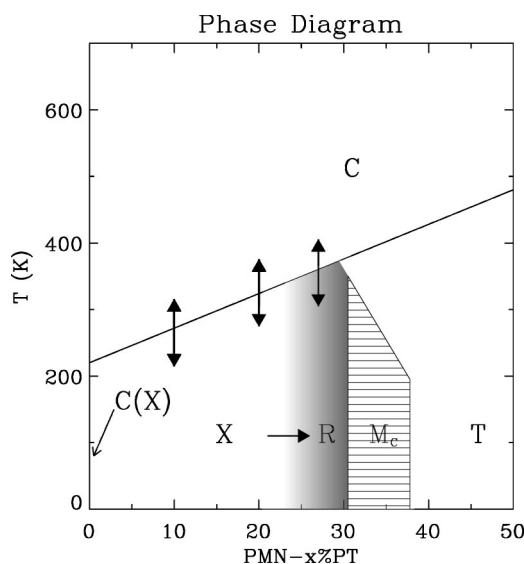


FIG. 1. Schematic of the revised phase diagram of PMN-xPT in zero field. The arrows indicate compositions that have been studied using high q -resolution neutron-scattering techniques.

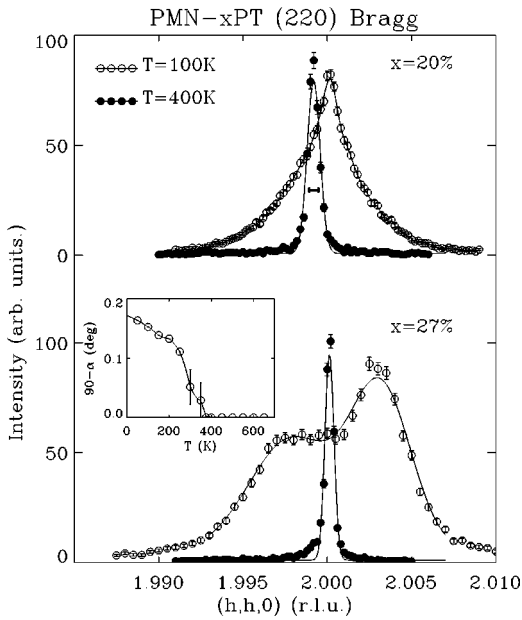


FIG. 2. Profiles of the (220) Bragg peaks for 20PT (top panel) and 27PT (bottom panel) are shown at 100 K (open circles) and 500 K (solid circles). The solid lines are fits described in the text. The horizontal bar indicates the q resolution along the (220) direction. The inset shows the temperature dependence of the rhombohedral angle α for the 27PT sample.

ergy E_i of 14.7 meV, obtained from the (002) reflection of a pyrolytic graphite (PG) monochromator and horizontal beam collimations of $10' - 46' - 20' - 40'$. We exploited the (004) reflection of a perfect Ge crystal as analyzer to achieve unusually fine q resolution near the relaxor (220) Bragg peak thanks to a nearly perfect matching of the sample and analyzer d spacings. Close to the (220) Bragg peak, the q resolution along the wave-vector direction is about 0.0012 \AA^{-1} ($\delta q/q \approx 2 \times 10^{-4}$).¹³

Figure 2 shows longitudinal ($\theta - 2\theta$) scans along the (220) pseudocubic Bragg peak both above and below T_C . The relative intensities have been scaled for ease of comparison. The Bragg profile for 20PT can be fit to a single peak at all temperatures and shows no evidence of any rhombohedral splitting. Above $T_C \sim 300$ K the profile fits well to a Gaussian line shape with a narrow width only slightly larger than that of the instrumental resolution. However the Bragg peak broadens considerably below T_C and is better described by a Lorentzian function. This broadening indicates the presence of a large internal strain within the crystal bulk below T_C .

By contrast, 27PT has a rhombohedral structure at low temperature. The (220) Bragg peak splits below $T_C \sim 375$ K, and is an unambiguous sign of the expected rhombohedral phase transition. The rhombohedral distortion increases on cooling, as shown by the plot of the rhombohedral angle α vs T (inset of Fig. 2).

These results clearly indicate that the low temperature phase of bulk 20PT is different from that of the rhombohedral phase observed in 27PT. The longitudinal full width at half maximum (2Γ) of the (220) Bragg peak is plotted versus temperature in Fig. 3 as is the lattice parameter a . Data

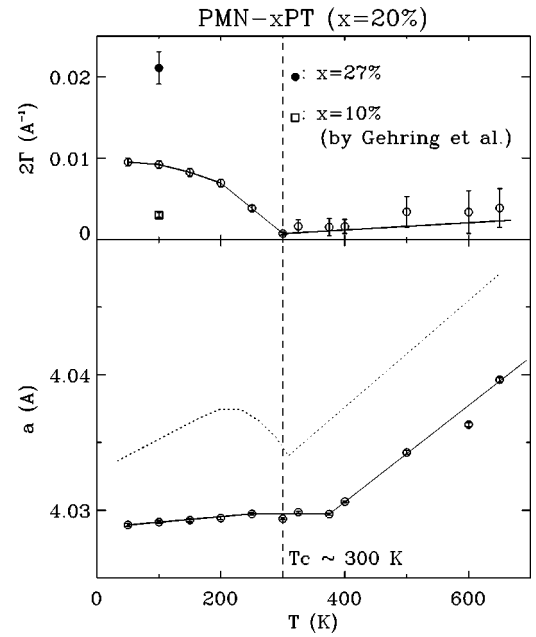


FIG. 3. Top panel: the resolution corrected Full width at half maximum (2Γ) of the (220) Bragg peak vs T for 20PT (open circles), compared with data from 27PT (close circle) and 10PT (square) by Gehring *et al.*¹¹ Bottom panel: lattice parameter a vs T . The dotted line represents thermal-expansion behavior typical of normal ferroelectrics. The solid lines are guides to the eye.

taken on heating and cooling yield similar results and thus no hysteretic effects. The 20PT Bragg profile is sharp and almost resolution limited at high temperature, but begins to broaden below $T_C \sim 300$ K, which is indicative of a true phase transition. For comparison, we also show the values of 2Γ at 100 K for the 27PT sample (solid circle) and the PMN-10PT sample (open rectangle) measured by Gehring *et al.*¹¹ Clearly the broadening develops not only with cooling, but also with increasing PT concentration.

For normal ferroelectric oxides, the lattice parameter decreases linearly on cooling down to T_C , then increases in the ferroelectric region, as shown by the dotted line in Fig. 3. In relaxors, the linearity breaks down at a temperature T_x above T_C . Experimental evidence for this have been provided by the independent measurements of Dkhil *et al.*¹² and Ye *et al.*⁷ on a series of PMN- x PT samples. The 20PT lattice parameter follows the linear behavior seen in conventional ferroelectrics at high temperature, but shows a break at $T_x \sim 380$ K, and remains almost constant below T_x . In addition, the unit-cell volume does not increase with cooling in the ferroelectric region. This anomalous feature is characteristic of phase X, and has also been observed in pure PMN (Refs. 14,12) and PMN-10PT.¹¹

Our results provide additional evidence that PMN- x PT transforms into phase X at low temperature for small PT concentrations. The studies by Ohwada *et al.*⁹ and Xu *et al.*¹⁰ provide compelling evidence that the same picture is true for PZN- x PT. By using x rays with different incident energies, Xu *et al.*¹⁰ also found out that the outermost $\sim 50 \mu\text{m}$ of the PZN crystal does exhibit a rhombohedral distortion. The thickness of the outer layer is estimated from the penetration

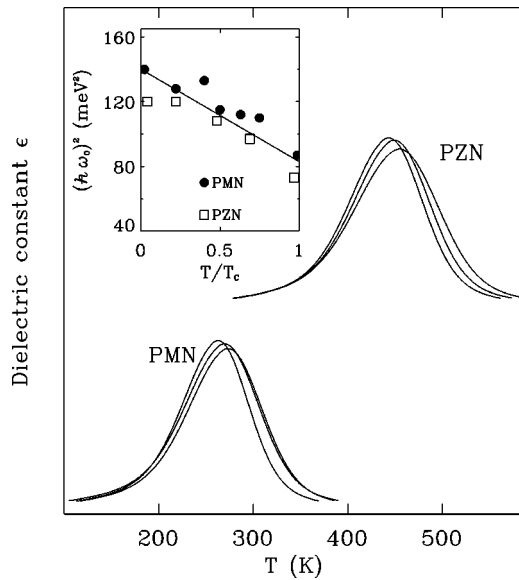


FIG. 4. A schematic comparison between PMN and PZN, showing the frequency dependent dielectric constant ϵ vs T . The inset shows the soft TO phonon energy squared vs T/T_C for PMN¹⁶ and PZN.¹⁵

depths of different x-ray energies, and may vary with different compounds. However, it is important to note that the existence of an outer layer with a structure different from that of the inside naturally explains the discrepancies between earlier x ray powder diffraction and the recent neutron and high-energy x-ray scattering results. And the fact that x-ray studies of pure PMN have not observed a rhombohedral phase could be understood if PMN represents the limiting case of phase X with a very thin outer layer.

Our results, together with other neutron-scattering measurements of phase X ,^{11,15} show that all measured Bragg peaks broaden significantly in the longitudinal direction below the Curie temperature T_C . These neutron results are in contrast to the high-energy x-ray case,¹⁰ where the Bragg profiles are sharp for temperatures both above and below T_C . We speculate that these differences are due to the fact that the incident neutron beam has a much larger size and divergence than the x-ray beam, therefore more sensitive to the inhomogeneity of the whole crystal. More measurements are currently underway for better understanding of these differences.

In phase X , the crystal lattice is undistorted, and the Bragg peaks do not split in diffraction measurements. However, the true symmetry is not yet determined. To get detailed information on average atomic positions, we are planning further investigations on refinements from single-crystal diffractions. Unfortunately, extinction effects arising from those near-perfect crystals are making this quite difficult.

Both PMN and PZN are relaxors that exhibit a broad and strong frequency-dependent dielectric constant ϵ as shown in Fig. 4. Despite the absence of a rhombohedral distortion in phase X , ferroelectric polar order is still present in the system. Recently, neutron inelastic scattering measurements by Wakimoto *et al.*¹⁶ of the ferroelectric soft TO phonon in pure PMN revealed that the soft mode recovers at temperatures

below $T_C \sim 213$ K. Similar measurements on PZN were later performed by Stock *et al.*,¹⁵ where $T_C \sim 410$ K. The linear relationship between the soft TO phonon energy squared $(\hbar\omega_0)^2 \propto 1/\epsilon$ and T (see inset of Fig. 4) is a clear signature of an ordered ferroelectric phase below T_C .

In ferroelectric systems, the primary order parameter is the polarization \vec{P} caused by ionic shifts. It is usually coupled to a secondary-order parameter—the lattice distortion, which changes the shape of the unit cell and is more readily accessible by scattering methods. Recent reports on epitaxial films of SrTiO₃ and BaTiO₃¹⁷ show that this coupling is broken in these systems, possibly due to epitaxy strain and substrate clamping effects. The coexistence of ferroelectric spontaneous polarization and an undistorted lattice is an example of the decoupling inside a free-standing crystal.

In pure PMN, polar regions, with sizes of a few nanometers, start to form at the Burns temperature¹⁸ $T_d \approx 600$ K, and contribute directly to diffuse scattering.^{19,20} Both neutron and x-ray measurements^{12,21–23} show that in relaxors, the diffuse scattering intensity starts to be visible around T_d , and increases monotonically on cooling. An important step in understanding the nature of these polar nanoregions (PNR) has been made by Hirota *et al.*,²⁴ with the concept of phase-shifted PNR. The atomic displacements derived from previous neutron diffuse scattering data on PMN (Ref. 25) by Vakhrušev *et al.* were reexamined and decomposed into the sum of two terms with comparable magnitudes. The first term satisfies the center-of-mass condition and is consistent with the values derived from inelastic-scattering intensities from the soft TO mode.^{16,26} The second term represents a uniform shift along the polar directions of the PNR relative to the surrounding lattices. In this picture, the PNR condense from the soft TO mode, and exhibit a “uniform phase shift,” or displacement, below T_d . Experimental evidence of this uniform phase shift has been observed by Gehring *et al.*²⁷ by applying an external electric field along the [001] direction of a PZN-8PT single crystal. The diffuse scattering intensity around the (003) Bragg peak is considerably reduced at all temperatures below T_C , while the diffuse scattering around (300) remains strong. The size of this phase shift is comparable to the first term and is estimated to be around 1/10 of the lattice spacing. This large phase shift creates a huge energy barrier, making it extremely difficult for the PNR to merge into the surrounding lattice.

The interaction between the PNR and the surrounding lattice can be viewed as a coupling parameter between the ferroelectric polarization and lattice distortion. We conjecture that the balance between the energy barrier caused by the uniform phase shift and this coupling parameter is the key in understanding phase X . For $T < T_C$, the entire system is polarized. Nevertheless, in order for a long range rhombohedral distortion to develop, the energy barrier must be overcome before the PNR can merge and grow into macroscopic rhombohedrally distorted domains. This can only be achieved when the interaction between the PNR and the surrounding environment is sufficiently strong. Otherwise, the lattice will remain undistorted, with confined ferroelectric polarization.

In other words, phase X is a special confined form of rhombohedral phase. Electric-field studies on PZN-8PT by Ohwada *et al.*⁹ confirm this by showing that phase X always transforms into the M_A phase first with increasing field, following the polarization rotation path of $R \rightarrow M_A \rightarrow M_C \rightarrow T$, indicating a $\{111\}$ rhombohedral type of polarization in phase X .

The confinement of local rhombohedral order in phase X inevitably induces instability in the system. The interaction between the PNR and the surrounding undistorted lattice creates strain and stress in the system, which leads to the broadening of the Bragg profile below T_C . A small external “force” may be able to drive the whole system into a more stable phase. For example, by application of a small electric

field, even pure PMN can be transformed into a rhombohedral phase below T_C .²⁸ With increasing PT concentration, the coupling becomes stronger and the instability increases. Eventually, the “confinement” breaks down and the usual coupling between rhombohedral distortion and ferroelectric polarization is reestablished for larger PT concentrations.

We would like to thank C. Stock and S. B. Vakhrušev for stimulating discussions, and H. C. Materials for providing the single crystals. Financial support from the U.S. Department of Energy under Contract No. DE-AC02-98CH10886 and Office of Naval Research under Contract Nos. N000140210340, N000140210126, and MURI N000140110761 is also gratefully acknowledged.

-
- ¹S.-E. Park and T.R. Shrout, *J. Appl. Phys.* **82**, 1804 (1997).
²J. Kuwata, K. Uchino, and S. Nomura, *Ferroelectrics* **37**, 579 (1981).
³B. Noheda, D.E. Cox, G. Shirane, J. Gao, and Z.-G. Ye, *Phys. Rev. B* **66**, 054104 (2002).
⁴D. La-Orauttapong, B. Noheda, Z.-G. Ye, P.M. Gehring, J. Toulouse, D.E. Cox, and G. Shirane, *Phys. Rev. B* **65**, 144101 (2002).
⁵P. Bonneau, P. Garnier, E. Husson, and A. Morell, *Mater. Res. Bull.* **24**, 201 (1989).
⁶N. de Mathan, E. Husson, G. Calvarin, J.R. Gavarri, A.W. Hewat, and A. Morell, *J. Phys.: Condens. Matter* **3**, 8159 (1991).
⁷Z.-G. Ye, Y. Bing, J. Gao, A.A. Bokov, P. Stephens, B. Noheda, and G. Shirane, *Phys. Rev. B* **67**, 104104 (2003).
⁸A. Lebon, H. Dammak, G. Calvarin, and I.O. Ahmedou, *J. Phys.: Condens. Matter* **14**, 7035 (2002).
⁹K. Ohwada, K. Hirota, P.W. Rehrig, Y. Fujii, and G. Shirane, *Phys. Rev. B* **67**, 094111 (2003).
¹⁰G. Xu, Z. Zhong, Y. Bing, Z.-G. Ye, C. Stock, and G. Shirane, *Phys. Rev. B* **67**, 104102 (2003).
¹¹P.M. Gehring, W. Chen, Z.-G. Ye, and G. Shirane, *cond-mat/0304289* (unpublished).
¹²B. Dkhil, J.M. Kiat, G. Calvarin, G. Baldinozzi, S.B. Vakhrušev, and E. Suard, *Phys. Rev. B* **65**, 024104 (2001).
¹³Details of the high q -resolution neutron-scattering technique will be discussed elsewhere.
¹⁴J. Zhao, A.E. Glazounov, Q.M. Zhang, and B. Toby, *Appl. Phys. Lett.* **72**, 1048 (1998).
¹⁵C. Stock, R.J. Birgeneau, S. Wakimoto, J. Gardner, W. Chen, Z.-G. Ye, and G. Shirane, *cond-mat/0301132* (unpublished).
¹⁶S. Wakimoto, C. Stock, R.J. Birgeneau, Z.-G. Ye, W. Chen, W.J.L. Buyers, P.M. Gehring, and G. Shirane, *Phys. Rev. B* **65**, 172105 (2002).
¹⁷F. He, B.O. Wells, S.M. Shapiro, M.v. Zimmermann, A. Clark, and X.X. Xi, *Appl. Phys. Lett.* **83**, 123 (2003).
¹⁸G. Burns and F.H. Dacol, *Phys. Rev. B* **28**, 2527 (1983).
¹⁹A. Naberezhnov, S. Vakhrušev, B. Doner, D. Strauch, and H. Moudden, *Eur. Phys. J. B* **11**, 13 (1999).
²⁰S.B. Vakhrušev, B.E. Kvyatkovskiy, A.A. Naberezhnov, N.M. Okuneva, and B. Toperverg, *Ferroelectrics* **90**, 173 (1989).
²¹H. You and Q.M. Zhang, *Phys. Rev. Lett.* **79**, 3950 (1997).
²²D. La-Orauttapong, J. Toulouse, J.L. Robertson, and Z.-G. Ye, *Phys. Rev. B* **64**, 212101 (2001).
²³T.Y. Koo, P.M. Gehring, G. Shirane, V. Kiryukhin, S.-G. Lee, and S.-W. Cheong, *Phys. Rev. B* **65**, 144113 (2002).
²⁴K. Hirota, Z.-G. Ye, S. Wakimoto, P.M. Gehring, and G. Shirane, *Phys. Rev. B* **65**, 104105 (2002).
²⁵S.B. Vakhrušev, A.A. Naberezhnov, N.M. Okuneva, and B.N. Savenko, *Phys. Solid State* **37**, 1993 (1995).
²⁶P.M. Gehring, S. Wakimoto, Z.-G. Ye, and G. Shirane, *Phys. Rev. Lett.* **87**, 277601 (2001).
²⁷P. M. Gehring *et al.*, *cond-mat/0307513* (unpublished).
²⁸G. Calvarin, E. Husson, and Z.-G. Ye, *Ferroelectrics* **165**, 349 (1995).